BC
Co

Dimensional Stability of Fused Silica, Invar, and Several Ultralow Thermal Expansion Materials

J. W. Berthold III, S. F. Jacobs, and M. A. Norton*

Optical Sciences Center, University of Arizona, Tucson, Arizona 85721

ABSTRACT

We have measured length change vs time for several low thermal expansion materials maintained in evacuated environments at constant temperature (near 300 K). Materials were two types of fused silica, Cer-Vit, ULE, Zerodur, Invar, and Super Invar. $\Delta L/L$ was measured over a period of 170 days to a precision of two to three parts in 10^9. In addition, we have measured time-dependent changes in optical contact interfaces and have placed an upper limit on drift of optical phase shift on reflection from multilayer dielectric coatings.

*Now with the Department of Physics, California Polytechnic State University, San Luis Obispo, California 93407.

1. INTRODUCTION

Extremely stable structures are becoming increasingly important in metrology, geophysics, and space exploration, where precise systems must operate unattended for long periods of time. In recent years, a number of materials have been developed that are dimensionally stable against temperature changes. These include Owens-Illinois Cer-Vit C-101, Corning ULE 7971, and Schott Zerodur, whose thermal expansion coefficients are exceedingly low over a wide temperature interval around room temperature (see Fig. 1). It is of further interest to determine the dimensional stability of these materials with the passage of time at constant temperature.

Ben Justice, in collaboration with the National Bureau of Standards, studied with Fizeau interferometry the average dimensional stability of nine one-in. blocks of the following materials: Corning ULE 7971 (titanium silicate), Corning glass-ceramic (two kinds), and Corning 7940 fused silica.[1] Measurements were performed during a three three-year period (1969-1972) with an accuracy of 0.012 fringe, corresponding to $\Delta L/L$ of a few parts in 10^7. Justice's results are summarized in Table I.

Recently, dimensional stability measurements of Cer-Vit and ULE were made by Bruce and Duffy at Commonwealth Scientific and Industrial Research Organization.[2] Their technique involved optically contacting Fabry-Perot mirrors to both ends of each 5-cm sample and illuminating them with Kr^{86} radiation.[3] Changes in length of one part in 10^8 were detected by monitoring fringe diameters over a 90-day period. These

measurements are summarized in Table I and are compared with our results and those of Justice. To account for nonbulk contributions (changes in optical phase shift on reflection and optical contact interface separation) Bruce and Duffy performed an auxiliary experiment: Two highly reflecting endplates, one with a flat surface and one with curvature, were optically contacted to form a "zero-spacer" etalon. This etalon exhibited long-term optical path length change $\Delta L/L$ of about -2×10^{-8} over 30 days, not unlike changes we observed for optical contacts over the same period. Bruce and Duffy, however, did not attempt to separate optical contact changes from changes in phase shift on reflection.

More recently, U. E. Hochuli et al.[4] at the University of Maryland reported dimensional stability of Corning 99JJW low-expansion material. Their method involves constructing a Fabry-Perot etalon, similar to that of Bruce and Duffy, slaving a laser to the cavity resonant frequency, and then comparing the slave laser frequency with that of a frequency-stabilized laser. This technique should be limited only by the stability of the second laser $\Delta\nu/\nu = -\Delta L/L \approx 5 \times 10^{-9}$ for the Spectra Physics Model 119. No attempt was made to evaluate changes due to surface effects.

The fact that low thermal expansion materials change length with time as much as 1 ppm over a three-year period led NASA to initiate the present measurement program, in collaboration with the National Bureau of Standards, Corning Glass Works, and the University of Maryland. The purpose of this program was to measure with increased accuracy, over a period of time shorter than three years, the dimensional stability of the

above-mentioned materials. In addition to the three ultralow expansion materials, Heraeus-Schott Homosil was included in the study because Sakuma of Bureau International de Poids et Mesures reported great dimensional stability for this material. This, in turn, raised the question of whether Corning's fused silica (7940) was any less stable. At the suggestion of Dr. Charles Freed of MIT, the Arizona group included in its study Universal Cyclops Invar LR-35 and Simonds Saw and Steel Company Super Invar. These materials are also used in applications where length invariance is important. In a nutshell, our measurements of ULE agree well with those of Bruce and Duffy, but not as well with those of Justice, probably because of inhomogeneity and/or small temporal optical contact shrinkage among his nine samples. While our measurements of fused silica agree with those of Justice, as shown in Table I, for Cer-Vit we obtain one-third the Bruce and Duffy value. This discrepancy probably occurs because of the differential expansivity between the Cer-Vit etalon spacer and fused silica endplates used by Bruce and Duffy.

In common with Bruce and Duffy and with Hochuli, the method we used to study length change is based on Fabry-Perot interferometry. The sample serves as the spacer, with highly reflecting mirrors optically contacted to both ends of the sample as shown in Fig. 2. When the spacer length L changes by an amount ΔL, the Fabry-Perot resonances drift by an amount $\Delta\nu$, where

$$\Delta\nu/\nu = -\Delta L/L. \qquad (1)$$

More precisely, L in Eq. (1) should be replaced by the one-way optical

path length of the Fabry-Perot resonator, including not only the sample's physical length, but also the optical contact interface separation and the optical phase shift on reflection from the mirrors. Thus for correct evaluation of measurements of this kind it is necessary to be able to separate out the above surface effects from bulk effects, which obey a law $\Delta L \propto L_0$. This separation is not possible using a single Fabry-Perot resonator,[5] and we describe in the next section how the use of two Fabry-Perot resonators of identical material but different lengths makes possible separation of bulk from (combined) surface effects. Finally, we describe an auxiliary experiment that we performed to estimate the interface drift of an average optical contact (see Fig. 3). This, in turn, makes it possible to estimate the change in optical phase shifts. Details of the work described below are contained in the dissertation of J. Berthold.[6]

2. MEASUREMENT TECHNIQUE

Apparatus

The method of measurement is an outgrowth of a technique previously described for ultraprecise measurement of thermal expansion coefficients.[7] As shown in Fig. 4, a frequency stabilized laser beam is passed through a Fabry-Perot resonator (FP), which consists of the sample as spacer with confocal mirrors optically contacted to either end. Modulator KDP, driven by a variable frequency rf source, impresses tunable sidebands on the laser light, which are used to track the cavity resonances.

Unmodulated laser light is blocked by polarizer P, and the combination of P and quarterwave plate $\lambda/4$ attenuates reflections back

from the FP resonator into the laser. Sample cavities are maintained in temperature-controlled ovens O. Light transmitted by the cavities at resonance is monitored by detector D, whose output is displayed on an oscilloscope screen CRO. When the FP optical path length changes for any reason, the subsequent shift in cavity resonance is tracked by the movable sidebands and measured by frequency counter FC.

At first, we experienced difficulty in obtaining adequately reproducible measurements of cavity resonant frequency. The resonant frequencies varied with mode matching lens position, because the round-trip cavity optical path length depends on the degree of off-axis illumination.[8] We finally achieved reproducibility, at the expense of some throughput, by adding a 0.6-mm-diameter aperture and eliminating the matching lens.

To reduce noise due to air pressure fluctuations within each FP resonator, all samples were maintained in a vacuum continuously less than 300 mTorr. Cryogenic pumps were used to avoid sample contamination by pump vapors.

Two-Cavity Method

To separate surface effects (optical contact drift and phase shifts) from bulk effects ($\Delta L \propto L$), we fabricated a long (10 cm) and a short (8 cm) etalon of each material. If we assume identical material and a length change $\Delta L \propto L$, then the frequency shifts $\Delta\nu/\nu$ should be the same, irrespective of cavity length (see Eq. (1)). We must expect, however that surface effects also change with time in a manner quite independent of L. Let us denote such contact and phase-shift changes with time and

temperature as $\Delta\phi(t,T)$. Then we may define a temporal dimensional stability coefficient at constant temperature

$$\alpha_t \equiv \frac{1}{L}\left(\frac{\Delta L}{\Delta t}\right)_T \tag{2}$$

analogous to the thermal expansion coefficient

$$\alpha_T \equiv \frac{1}{L}\left(\frac{\Delta L}{\Delta T}\right)_t . \tag{3}$$

Generalizing Eq. (1) to read optical path length instead of L, and using Eqs. (2) and (3), we obtain

$$\frac{\Delta\nu}{\nu} = -\frac{\alpha_T\Delta T + \alpha_t\Delta t + (\lambda/2\pi L)\Delta\phi(t,T)}{1 + (\lambda/2\pi L)\phi(t_0,T_0)} . \tag{4}$$

Measurement of $\Delta\nu/\nu$ for long vs short cavities makes possible evaluation of $\Delta\phi(t,T)$, the changes in lumped optical phase shift. Designating the long and short cavities by subscripts L and S

$$\frac{\Delta\nu_L - \Delta\nu_S}{\nu} = -(\alpha_T\Delta T + \alpha_t\Delta t)\left\{\left[1 + \frac{\lambda}{2\pi}\frac{\phi(t_0,T_0)}{L_L}\right]^{-1} - \left[1 + \frac{\lambda}{2\pi}\frac{\phi(t_0,T_0)}{L_S}\right]^{-1}\right\}$$

$$- \frac{\lambda}{2\pi}\Delta\phi(t,T)\left(\left\{L_L\left[1 + \frac{\lambda}{2\pi}\frac{\phi(t_0,T_0)}{L_L}\right]\right\}^{-1}\right.$$

$$\left. - \left\{L_S\left[1 + \frac{\lambda}{2\pi}\frac{\phi(t_0,T_0)}{L_S}\right]\right\}^{-1}\right) . \tag{5}$$

It is shown in Appendix A that the first term on the right-hand side is negligible compared to our experimental error of 10^{-9}. Thus Eq. (5) can be solved for $\Delta\phi$ and, using the fact that $\phi(t_0,T_0) < \pi$,

$$\Delta\phi(t,T) \simeq \frac{2\pi}{c} \frac{L_L L_S}{L_S - L_L} (\Delta\nu_L - \Delta\nu_S), \tag{6}$$

where c is the velocity of light and L_L and L_S were determined to one part in 10^4, using Browne and Sharp gauge blocks. This means that $\Delta\phi$ can be measured to that accuracy. (Another order of magnitude is achievable by measuring $c/2L$ using laser beam sidebands for probes and improved dielectric coatings.)

We show below that, when the time-dependent slopes of cumulative frequency change vs time for long and short sample pairs become equal, these slopes measure the dimensional stability of the materials. Equation (6) may be rewritten

$$\Delta\phi(t,T) \simeq -\frac{2\pi}{c} L_L \Delta\nu_L^{\phi}, \tag{7}$$

where

$$\Delta\nu_L^{\phi} \simeq \frac{L_S}{L_L - L_S} (\Delta\nu_L - \Delta\nu_S). \tag{8}$$

$\Delta\nu_L^{\phi}$ in Eq. (7) is that part of the change in resonant frequency of the long cavity due to changes in surface effects.

In Appendix B it is shown that the total time-dependent resonant frequency change $\Delta\nu_L$ is approximately equal to the sum of the time-dependent resonance changes due to bulk change, $\Delta\nu_L^{D}$, and surface effects, $\Delta\nu_L^{\phi}$.

$$\Delta\nu_L = \Delta\nu_L^D + \Delta\nu_L^\phi. \tag{9}$$

Similarly, for the short cavity,

$$\Delta\nu_S = \Delta\nu_S^D + \Delta\nu_S^\phi. \tag{10}$$

If, during a period of time, the slopes $\Delta\nu/\Delta t$ for long and short cavities become equal,

$$\Delta\nu_L/\Delta t = \Delta\nu_S/\Delta t, \tag{11}$$

then

$$\Delta\nu_L^D + \Delta\nu_L^\phi = \Delta\nu_S^D + \Delta\nu_S^\phi. \tag{12}$$

Assuming our pairs are made of identical and homogeneous materials

$$\Delta\nu_L^D/\nu = \Delta\nu_S^D/\nu \tag{13}$$

so that

$$\Delta\nu_L^\phi = \Delta\nu_S^\phi. \tag{14}$$

But from Eq. (7), this means that

$$(c/2\pi L_L)\Delta\phi(t,T) = (c/2\pi L_S)\Delta\phi(t,T). \tag{15}$$

Finally we have assumed that all $\Delta\phi(t,T)$ are identical because all reflective coatings were deposited at the same time as identically as possible. Therefore, since L_L = 10 cm and L_S = 8 cm, Eq. (15) can hold only if

$$\Delta\phi(t,T) = 0 \tag{16}$$

for the time period where long and short cavity resonance frequency slopes $\Delta\nu/\Delta t$ are equal. During this period surface effects are no longer changing, leaving only the bulk effect $\alpha_t \Delta t$. Thus, when the slopes $\Delta\nu/\Delta t$ become equal for long and short cavities, this quantity measures the dimensional stability directly

$$\frac{1}{\nu}\frac{\Delta\nu}{\Delta t} = \alpha_t. \qquad (17)$$

Thermal Expansion

It is clearly desirable in these measurements to maintain each sample at a temperature where its thermal expansion is minimal. Figure 1 shows our measurements of α_T vs T for the seven materials of interest. In the case of Cer-Vit, Zerodur, and ULE, we were readily able to keep $\Delta L(T)/L < 10^{-9}$ with ±0.020°C temperature control. However, for the remaining samples, $\alpha \approx 5 \times 10^{-7}(C°)^{-1}$ at room temperature with zero thermal expansion occurring at inconveniently low temperatures. For these samples, we took the approach of maintaining constant temperature where we could control it best (±0.005°C long-term variation at room temperature) and correcting for small thermal changes using precise temperature measurement (±0.001°C) and precise knowledge of thermal expansion coefficients. Thus we kept $\Delta L(T)/L$ within one part in 10^9.

3. TREATMENT AND PREPARATION OF SAMPLES

Heat Treatment, Etching, and Handling

The five nonmetallic materials we studied were heat treated no less than 2.5 years prior to the beginning of our measurements. These

heat treatments, which are proprietary to the manufacturers, were all presumably standard, although our measurements of thermal expansion, which are strongly determined by heat treatment, indicate that Zerodur may have received a nonstandard heat treatment, i.e., unlike other Zerodur samples we have measured in the past, these samples exhibit no thermal expansion zero crossing near room temperature.

To relieve grinding and polishing stresses in the above materials, we etched each sample in hydrofluoric acid to a depth of 80 μm. Residual stress birefringence was less than 10 nm/cm.

The Invar and Super Invar samples were also identically heat treated about 2.5 years prior to measurement. The heat treatment is given in Table II. These materials were machined into annular cylinders between steps two and three of the heat treatment process. Since Invar materials are ferromagnetic alloys, great care was taken not to drop or jar the samples, nor to heat them above 100°C. These samples were shielded from magnetic fields in our ovens through the use of 0.25-mm-thick Co-Netic AA magnetic shield alloy. Magnetic fields were minimized through the use of bifilar, noninductive heater windings.

Multilayer Dielectric Coatings and Optical Contacts

All multilayer dielectric coatings were completed simultaneously on November 2, 1974. The coatings consisted of 21 quarterwave layers of ZnS and ThF_4 deposited alternately. The measured FWHM of the Fabry-Perot resonances varied from 3 to 10 MHz, indicating that the reflectivities (~99.5% at 633 nm) were not identical. The coated mirrors were

maintained under partial vacuum in a dessicator from their fabrication until optical contacts were made on May 28, 1975. The Fabry-Perot samples were then assembled in their oven enclosures, which were continuously maintained by cryosorption pumps at a pressure less than 300 mTorr. The total time the coatings were exposed to atmospheric pressure was about 10 hours during contacting and assembly.

To form Fabry-Perot etalons with the Invar materials (see Ref. 6), it was necessary to choose optically transparent endplate materials whose thermal expansion matched that of the Invar spacer. We used as a guideline for allowable mismatch tolerance 30×10^{-8} $(C°)^{-1}$, which, in our experience with thermal expansion measurement, corresponds to the onset of nonlinear distortions over a 10°C interval. We used Homosil endplates for the Invar etalons at 27°C, and Cer-Vit endplates for the Super Invar etalons at 28°C, corresponding to thermal expansion mismatches less than 7 and 9×10^{-8} $(C°)^{-1}$, respectively.

4. TEMPERATURE CONTROL AND MEASUREMENT

Oven Design and Temperature Control

Our oven design is based on an arrangement demonstrated by Williams,[9] who achieved microdegree temperature stability at 40°C for several days at the center of two concentric spherical ovens. Our cylindrical geometry precluded use of the spherical design. We therefore surrounded our massive copper sample holders with 6 cm of polyurethane insulation and placed this inside a cylindrical copper oven whose temperature was controlled by Yellow Springs Instrument Company

model 63RC controllers. This oven in turn was surrounded with 6 cm of the same insulation and placed inside a stainless steel cylinder (see Fig. 5). The entire assembly was situated in a cold environment supplied by a freezer (±0.5°C at 7°C). Due to differing heat leaks, not all our ovens performed equally well. Temperature stability ranged from ±0.005 to ±0.085°C. By locating the ultralow expansion samples, such as ULE, in the oven with poorest temperature regulation, and through knowledge of thermal expansion coefficients, we were able to correct for temperature-dependent length changes to one part in 10^9; that is, errors in thermal expansion coefficient compounded with uncertainty in temperature were kept negligible.

Temperature Measurement

Extremely important in dimensional stability measurement is the stability of the thermometer. Our primary thermometers were a pair of Rosemount platinum resistance thermometers (PRT) that we calibrated with a Jarrett Instrument Company triple-point-of-water cell and placed with the relatively high expansion, fused silica samples. All remaining samples were monitored by two Thermometrics, Inc. thermistors, one at either end of each copper cylinder (fused silica samples were monitored by one thermistor and one PRT). PRT units similar to ours were used for moonshot experiments and have been calibrated by the National Bureau of Standards and found stable to 0.002°C over five years. The thermistors, which were sealed in glass envelopes and aged, were selected by the manufacturers to have stability no worse than

0.005°C/year. This temperature uncertainty times the thermal expansion coefficient yielded uncertainty $\Delta L(T)/L < 10^{-9}$ for all our samples except Invar LR-35. In that particular case, the dimensional stability proved so large (see Table I) that the thermal drift uncertainty proved negligible (<0.2%). The above estimates of thermometer stability were verified when the ovens were dismantled and the thermometers were recalibrated with the triple-point-of-water cell.

5. FREQUENCY STABILIZED LASER AND BEAM MODULATION

The iodine-stabilized ^{3}He-^{22}Ne laser system used was supplied to us by the National Bureau of Standards. This laser delivers about 100 μW of power at 633 nm and derives its stability from an intracavity absorption cell filled with $^{129}I_2$. As described by Schweitzer et al.,[10] the long-term frequency uncertainty $\Delta\nu/\nu$ is approximately 10^{-10}, due to error in day-to-day resetability. Laser stability is thus not a limiting error in our dimensional stability measurements.

Small modulation of the laser beam was achieved from 10 MHz to 1000 MHz utilizing an Isomet model EOLM 400X modulator. With a polarizer placed after the KDP crystal and crossed with respect to the laser beam's linear polarization, the light was amplitude modulated, with the carrier suppressed. The percent modulation may be calculated using (Yariv[11])

$$I_{\text{transmitted}}/I_{\text{incident}} = \sin^2\Gamma/2, \tag{18}$$

where $\Gamma = V_{\text{applied}}/V_{\lambda/2}$. For our KDP, $V_{\lambda/2}$ = 1800 V and V_{applied} = 50 V,

leading to 0.6% modulation, which agreed with the measured value. As shown in Fig. 6, the modulation depth is quite flat between 500 MHz and 1000 MHz. The large variations below that range were due to impedance mismatches resulting in voltages in excess of 50 V between KDP electrodes and to subsequent increased modulation.

6. RESULTS AND CONCLUSIONS

In Figs. 7a through 7g, we show the cumulative drift vs time of Fabry-Perot resonant frequencies for 8- and 10-cm samples of each material. Each data point has been corrected for the small temperature-dependent frequency shift, $\Delta\nu = \nu_{NBS}\,\alpha\Delta T$, where α is the thermal expansion coefficient, ΔT is the temperature difference with respect to the starting temperature, and $\nu_{NBS} = 4.736 \times 10^{14}$ Hz.

The results of the auxiliary experiment (Fig. 3) to estimate the average change in optical contact interface separation are shown in Fig. 8. The cumulative resonant frequency drift of the two resonators was compared and the difference divided by the number of extra optical contacts. This average drift is plotted vs time, and from this curve we see that the frequency drift due to an average contact asymptotically approaches about 10.5 MHz, corresponding to a decrease in average optical contact separation $\Delta L = -(\Delta\nu/\nu)L = -2.2$ nm. This value is approximately equal to the rms roughness of each optical surface. We observe also that the curve in Fig. 8 is similar to most of the curves in Figs. 7a through 7g during the first 60 days, and we conclude that the major contribution to the early changes is attributable to the optical contacts, rather than to the reflection phase shifts.

As explained in the discussion of the two-cavity method, when the slopes $\Delta\nu/\Delta T$ for long and short cavities become equal, this quantity measures the dimensional stability (Eq. (16)). Since, for long and short samples of Cer-Vit and Homosil, the slopes were equal for practically all measurements, it appears that surface effects were always negligible for these samples (see Figs. 7c and d). However, the slopes of the remaining curves (long versus short cavities, Figs. 7a, b, and e through g) are dissimilar during the first 60 days and then become equal. For these samples, we concluded that the early curvature is due to surface effects and, as described in the preceding paragraph, the major contribution to these surface effects resulted from a decrease in optical contact separation. The only exception to this interpretation is the 10-cm Invar LR-35 sample, which showed an apparent *increase* in optical contact separation. This anomaly was resolved when we took apart the sample oven and found that for this sample one of the endplates was only in partial optical contact. This caused the endplate to tilt and increase, rather than decrease, the Fabry-Perot optical path length.

In Fig. 9 we present a summary overlay of Figs. 7a through g. Here we have expressed the dimensional changes of the 8-cm samples in terms of normalized optical path length $\Delta(OP)/OP = -\Delta\nu_{L,S}/\nu$, where $OP = L_{L,S}$ + (surface effects). Table I summarizes in a single number the dimensional stability for the seven materials measured. This number corresponds to the asymptotic linear slope for each curve in Fig. 9.

The metallurgists and glass scientists we have consulted feel that a quantitative description of the mechanisms we have been observing will be extremely difficult. We outline below three results from our measurements that may be useful for future quantitative analysis.

(1) Zerodur and Cer-Vit are structurally similar materials; they are both glass cermics annealed in such a way that they have a room temperature thermal expansion zero crossing. However, their dimensional stability is quite different. For Zerodur, we obtain a daily length change in parts per billion of 0 ± 0.03; for Cer-Vit 0.50 ± 0.03.

(2) Invar LR-35 and Super Invar are both iron-nickel alloys with identical heat treatments. Invar LR-35 is composed of approximately 63.5% Fe and 36.5% Ni compared to Super Invar whose composition is 63.5% Fe, 31.0% Ni, and 5.5% Co. The addition of 5.5% Co to Super Invar not only causes this material to have a room temperature thermal expansion zero crossing, but also a daily length change of 0 ± 0.03 parts per billion compared to 5.64 ± 0.03 for Invar LR-35.

(3) We obtain no significant difference between the dimensional stability of our fused silica samples of Homosil and Corning 7940. The daily length change of Homosil in parts per billion is -0.56 ± 0.03 and that for Corning 7940 is -0.51 ± 0.03.

APPENDIX A

We wish to show that

$$(\alpha_T \Delta T + \alpha_t \Delta t)\left\{\left[1 + \frac{\lambda}{2\pi}\frac{\phi(t_0,T_0)}{L_L}\right]^{-1} - \left[1 + \frac{\lambda}{2\pi}\frac{\phi(t_0,T_0)}{L_S}\right]^{-1}\right\} << 10^{-9}. \tag{A.1}$$

We note that, for all materials involved, $\alpha_T \Delta T = \Delta L/L < 10^{-6}$. Our experience with $\alpha_t \Delta t$ is more limited, but based on the worst case measured by Justice, $\alpha_t \Delta t < 10^{-6}$. We therefore conclude that $(\alpha_T \Delta T + \alpha_t \Delta t) < 10^{-5}$.

Since $\phi(t_0,T_0) < \pi$, and $(\lambda/2\pi)[\phi(t_0,T_0)/L] << 1$, we can expand inequality (A.1) to read

$$(\alpha_T \Delta T + \alpha_t \Delta t)(1 - \lambda/2L_L + \ldots - 1 + \lambda/2L_S - \ldots) << 10^{-9}. \tag{A.2}$$

But $\lambda/2L < 10^{-5}$ for long and short cavities, so the left-hand side of inequality (A.2) $< 10^{-10}$.

APPENDIX B

From Eq. (4)

$$\Delta\nu/\nu = -\left[\alpha_T \Delta T + \alpha_t \Delta t + \frac{\lambda}{2\pi L}\Delta\phi(t,T)\right]\left[1 + \frac{\lambda}{2\pi L}\phi(t_0,T_0)\right]^{-1} \tag{B.1}$$

but $\phi(t_0,T_0) < \pi$ and $\lambda/2L << 1$. Therefore

$$\Delta\nu/\nu \simeq -\left[\alpha_T \Delta T + \alpha_t \Delta t + \frac{\lambda}{2\pi L}\Delta\phi(t,T)\right]. \tag{B.2}$$

We can ignore the thermal term, $\alpha_T \Delta T$, since we have prior knowledge of the thermal expansion, and correct for length changes due to temperature change. Then

$$\Delta\nu/\nu \simeq -\left[\alpha_t \Delta t + \frac{\lambda}{2\pi L}\Delta\phi(t,T)\right] \tag{B.3}$$

and we recognize the first term on the right

$$\alpha_t \Delta t = \Delta L(t)/L \simeq -\Delta\nu^D/\nu \tag{B.4}$$

where $\Delta\nu^D$ is the time-dependent bulk length change contribution to the optical path length change. Finally, using Eq. (7) and Eq. (B.4), Eq. (B.3) can be written

$$\Delta\nu/\nu \simeq \Delta\nu^D/\nu - \frac{\lambda}{2\pi L}\left(-\frac{2\pi L}{c}\Delta\nu^\phi\right) \tag{B.5}$$

so that

$$\Delta\nu \simeq \Delta\nu^D + \Delta\nu^\phi. \tag{B.6}$$

ACKNOWLEDGMENTS

We would like to thank Dr. Charles Freed for supplying the Invar and Super Invar samples, Drs. Richard Deslattes and James Whetstone for supplying and helping us with the iodine stabilized laser, Mr. Richard Sumner for optical fabrication and especially for the difficult optical contacting, Mr. John Poulos for the optical coatings, and Prof. Roland V. Shack for numerous useful discussions. This work was supported in part by NASA, Marshall Space Flight Center, and Air Force Space and Missile Systems Organization under Contract FO4701-75-C-0248.

REFERENCES

1. B. Justice, "Dimensional Stability of Four Mirror Materials, Concluding Report," Corning Glass Works, Corning, New York (June 1972).
2. C. F. Bruce, Commonwealth Scientific and Industrial Research Organization, private communcation to the author, 1975.
3. C. F. Bruce and R. M. Duffy, Appl. Opt. 9(3):743-747 (1970).
4. U. E. Hochuli, P. Haldemann, and H. A. Li, Rev. Sci, Instr. 45(11): 1378-1381 (1974).
5. S. F. Jacobs, M. Norton, and J. W. Berthold III, "Dimensional Stability of Fused Silica and Several Ultralow Expansion Materials," International Symposium on Thermal Expansion of Solids (November 1973).
6. J. W. Berthold III, "Dimensional Stability of Low Expansivity Materials--Time Dependent Changes in Optical Contact Interfaces and Phase Shifts on Reflection from Multilayer Dielectrics," PhD Dissertation, University of Arizona, Tucson, Arizona, 1976.
7. S. F. Jacobs, J. N. Bradford, and J. W. Berthold III, Appl. Opt. 9(11):2477-2480 (1970).
8. Michael Hercher, Appl. Opt. 7(5):951-966 (1968).
9. James M. Williams, "Temperature Controlling to Micro-degrees," MIT Education Research Center (October 1971).
10. W. G. Schweitzer, Jr., E. G. Kessler, Jr., R. D. Deslattes, H. P. Layer, and J. R. Whetstone, Appl. Opt. 12(12):2927-2938 (1973).

11. Amnon Yariv, *Quantum Electronics* (New York, John Wiley and Sons, 1967), p. 311.

FIGURE CAPTIONS

Fig. 1. Thermal expansion coefficients measured at the University of Arizona for dimensional stability materials.

Fig. 2. Unequal-length Fabry-Perot resonators in evacuated copper housing (left), parts shown disassembled in photo.

Fig. 3. Two Fabry-Perot etalons, one with 12 optical contacts, the other with 2; used to measure the average change in optical contact interface separation.

Fig. 4. Schematic diagram of apparatus used to perform dimensional stability measurements. Mirror M_2 is translated as indicated by arrow to measure additional samples.

Fig. 5. Transverse and longitudinal cross-sectional views of stable oven.

Fig. 6. Relative sideband intensity vs modulation frequency.

Fig. 7. Cumulative resonant frequency change vs time: (a) Zerodur, (b) 7971 ULE, (c) Cer-Vit, (d) Homosil fused silica, (e) 7940 fused silica, (f) Super Invar, (g) LR-35 Invar.

Fig. 8. Cumulative resonant frequency change vs time due to an average optical contact drift.

Fig. 9. Normalized optical path-length change vs time for seven materials.

Table I

Average Daily Length Change $\Delta L/L$ (parts per billion)

Material	Justice	Bruce and Duffy	UA
Corning 7971 ULE titanium silicate	-0.38 ± 0.14	-0.2 ± 0.1	-0.17 ± 0.03
Corning 9623 glass ceramic	-0.32 ± 0.14	--	--
Corning 9622 glass ceramic	-1.09 ± 0.14	--	--
Corning 7940 fused silica	-0.50 ± 0.14	--	-0.51 ± 0.03
Owens-Illinois Cer-Vit C-101, glass ceramic	--	1.5 ± 0.1	0.50 ± 0.03
Heraeus-Schott Zerodur glass ceramic	--	--	0 ± 0.03
Heraeus-Schott Homosil fused silica	--	--	-0.56 ± 0.03
Universal Cyclops LR-35 Invar	--	--	5.64 ± 0.03
Simonds Saw & Steel Super Invar	--	--	0 ± 0.03

Table II

Heat Treatment Prescription

for LR-35 and Super Invar Samples

Step	Temperature (°C)	Time (hr)	Note
1	829	½	Water quench
2	316	1	Air cool
3	96	48	Air cool

Berthold et al.--Fig. 1

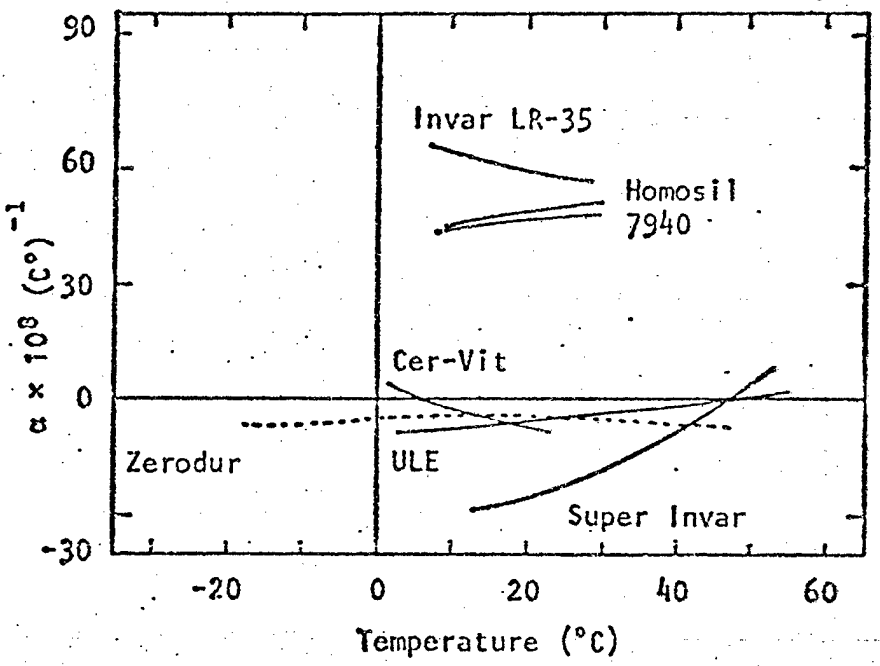

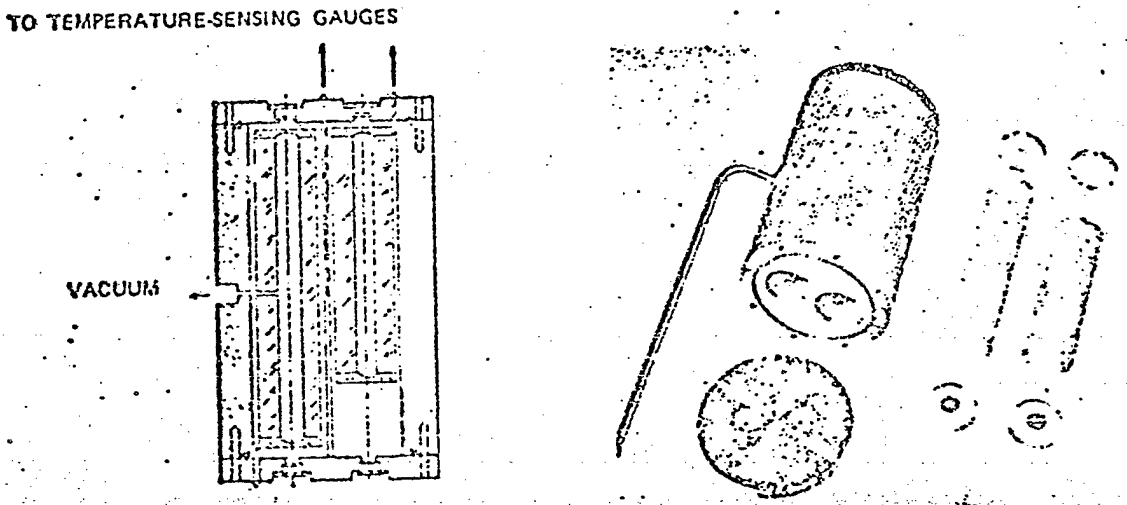
TO TEMPERATURE-SENSING GAUGES
VACUUM

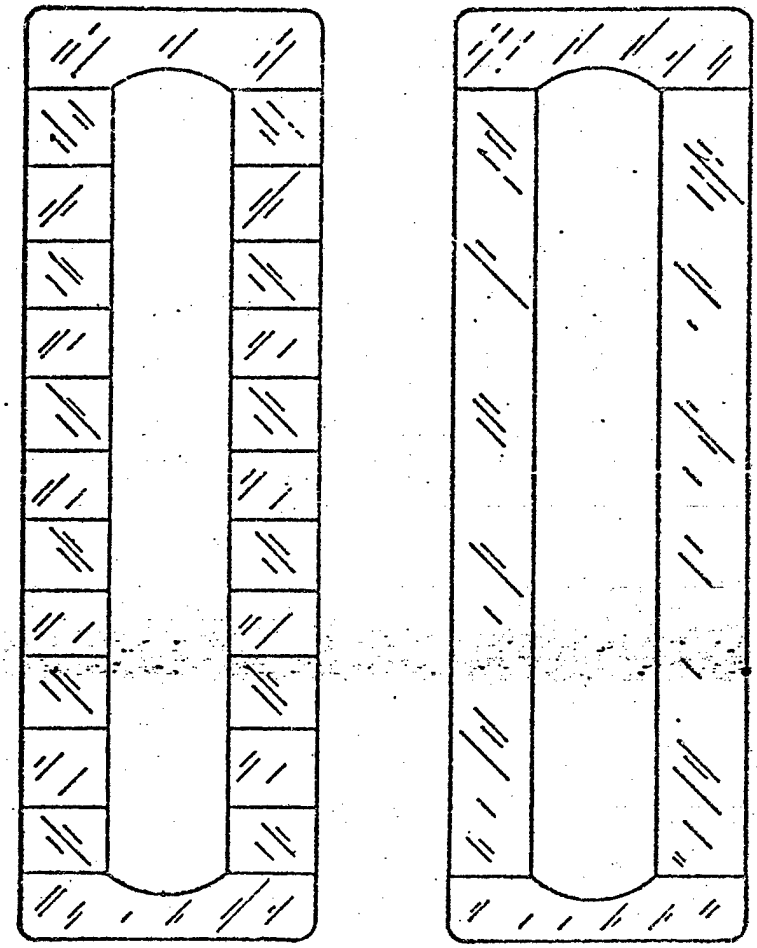

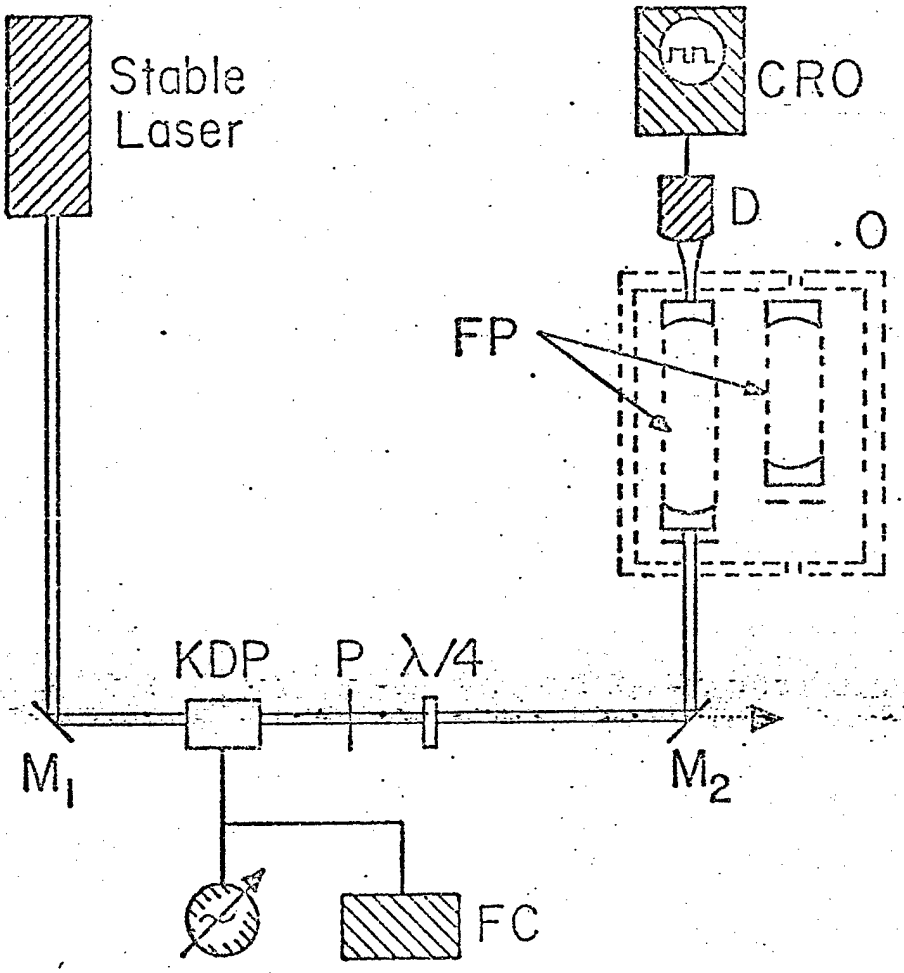
Stable
Laser
CRO
D
O
FP
KDP
P
λ/4
M1
M2
FC

Berthold et al.--Fig. 5

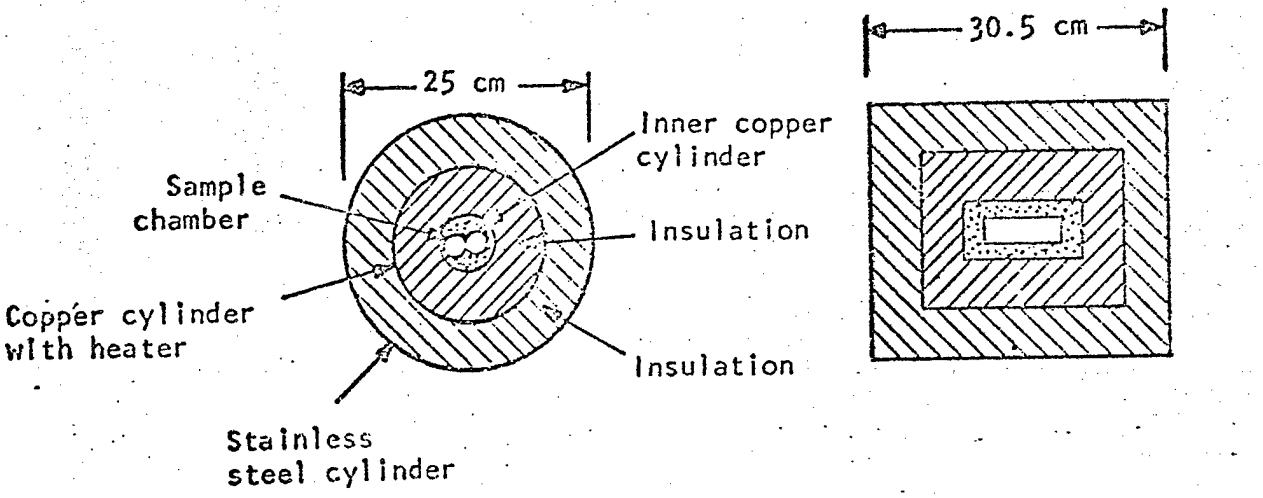

Transverse Cross Section

Longitudinal Cross Section

Berthold et al.--Fig. 6

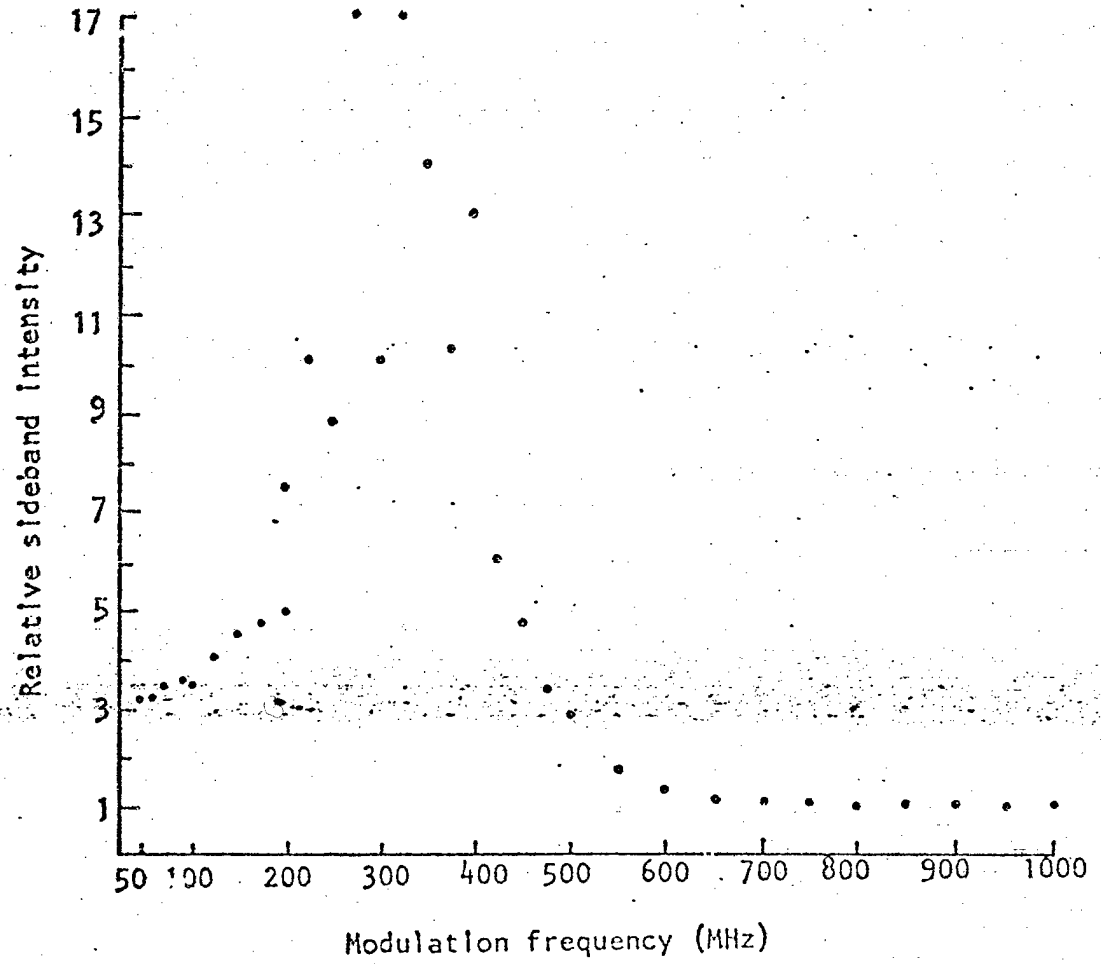

Berthold et al.--Fig. 7a

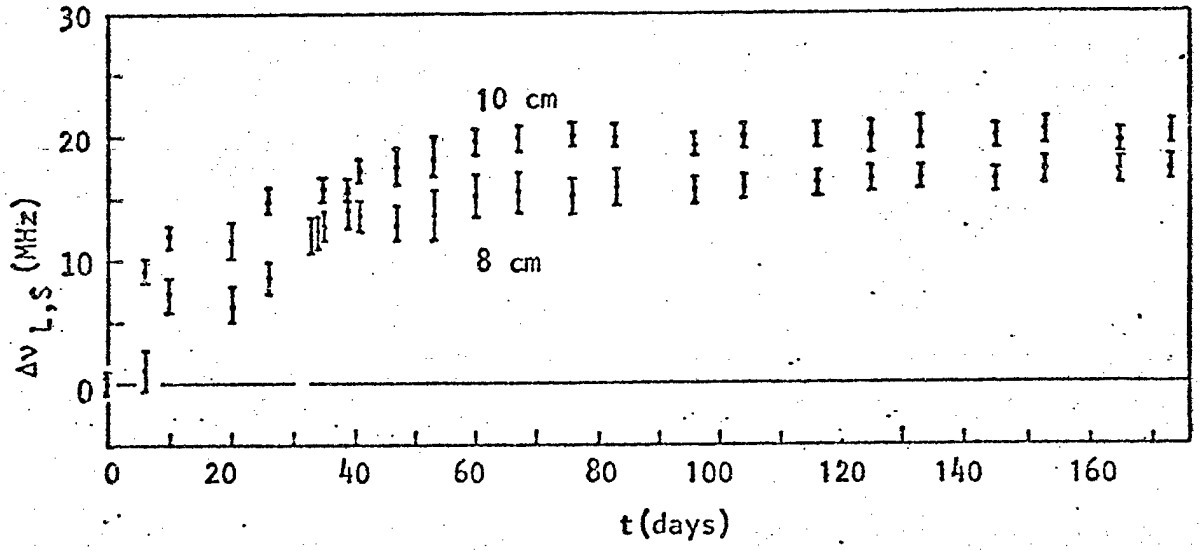

Berthold et al.--Fig. 7b

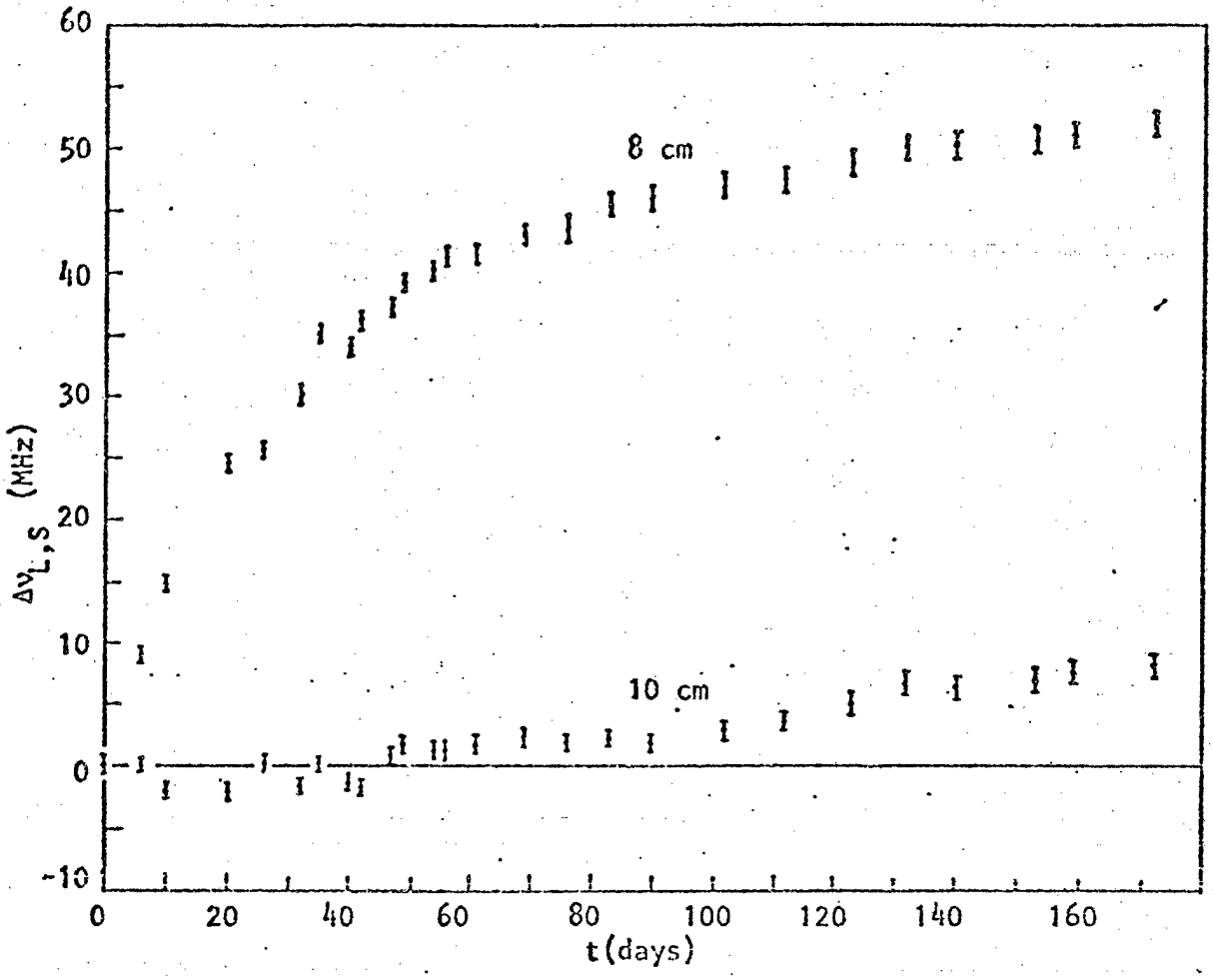

Berthold et al.--Fig. 7c

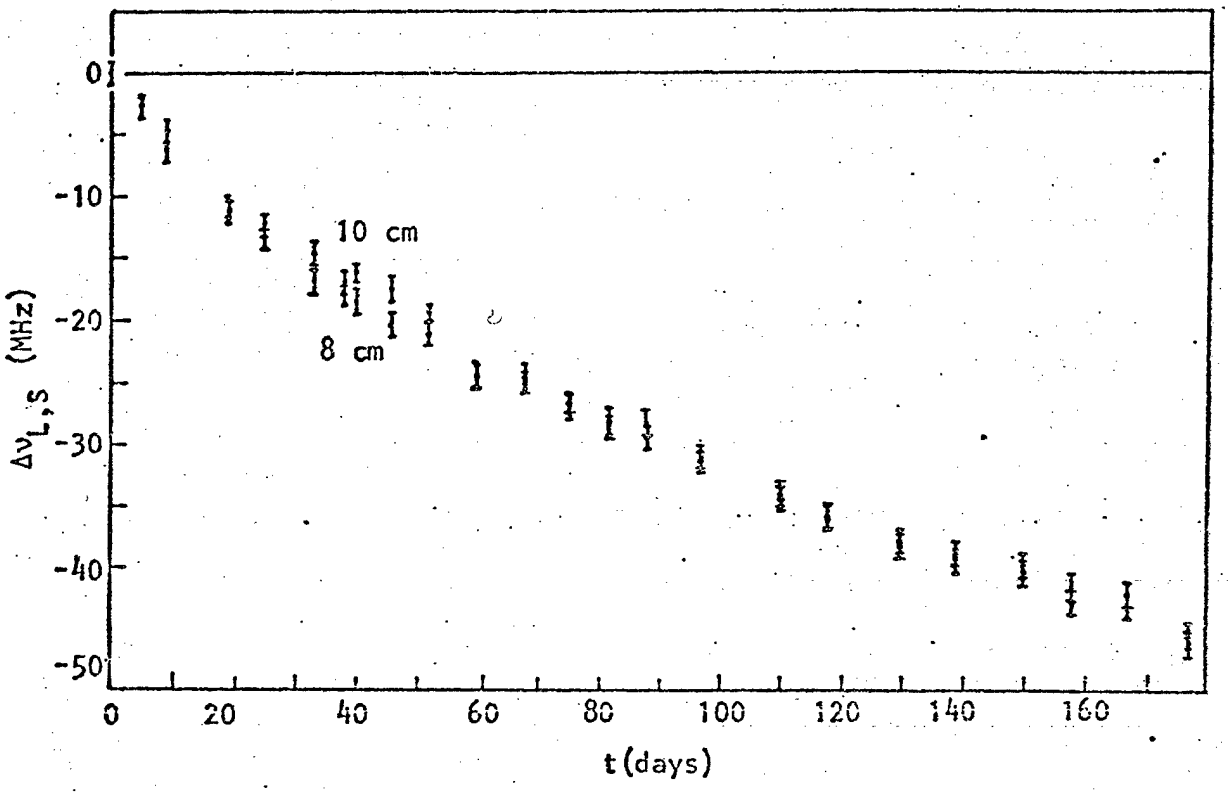

Berthold et al.--Fig. 7d

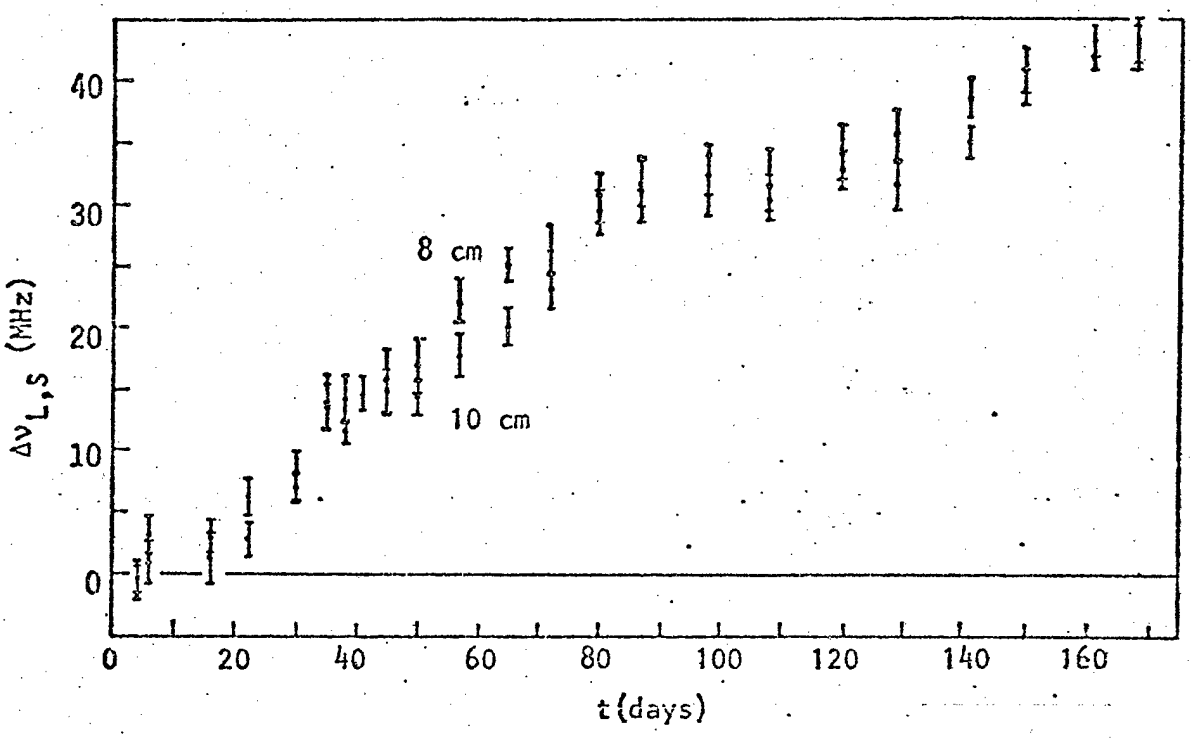

Berthold et al.--Fig. 7e

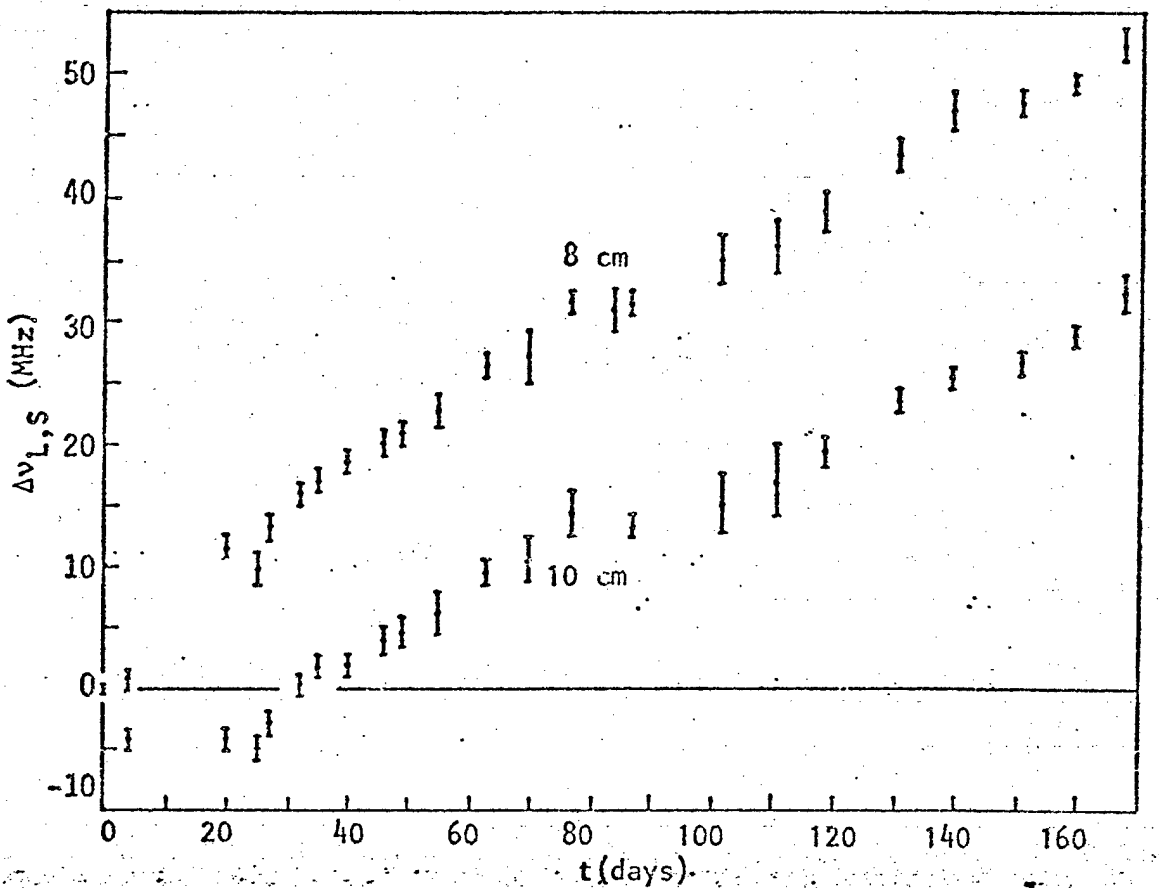

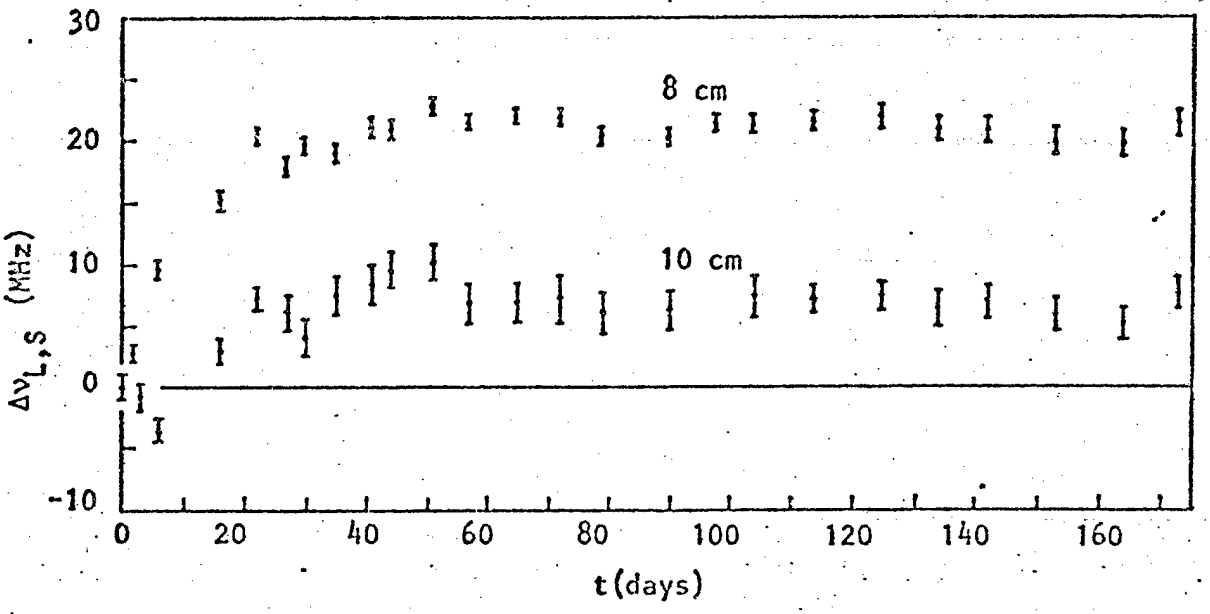
30
20
10
0
-10
8 cm
10 cm
$\Delta\nu_{L,S}$ (MHz)
0
20
40
60
80
100
120
140
160
t(days)

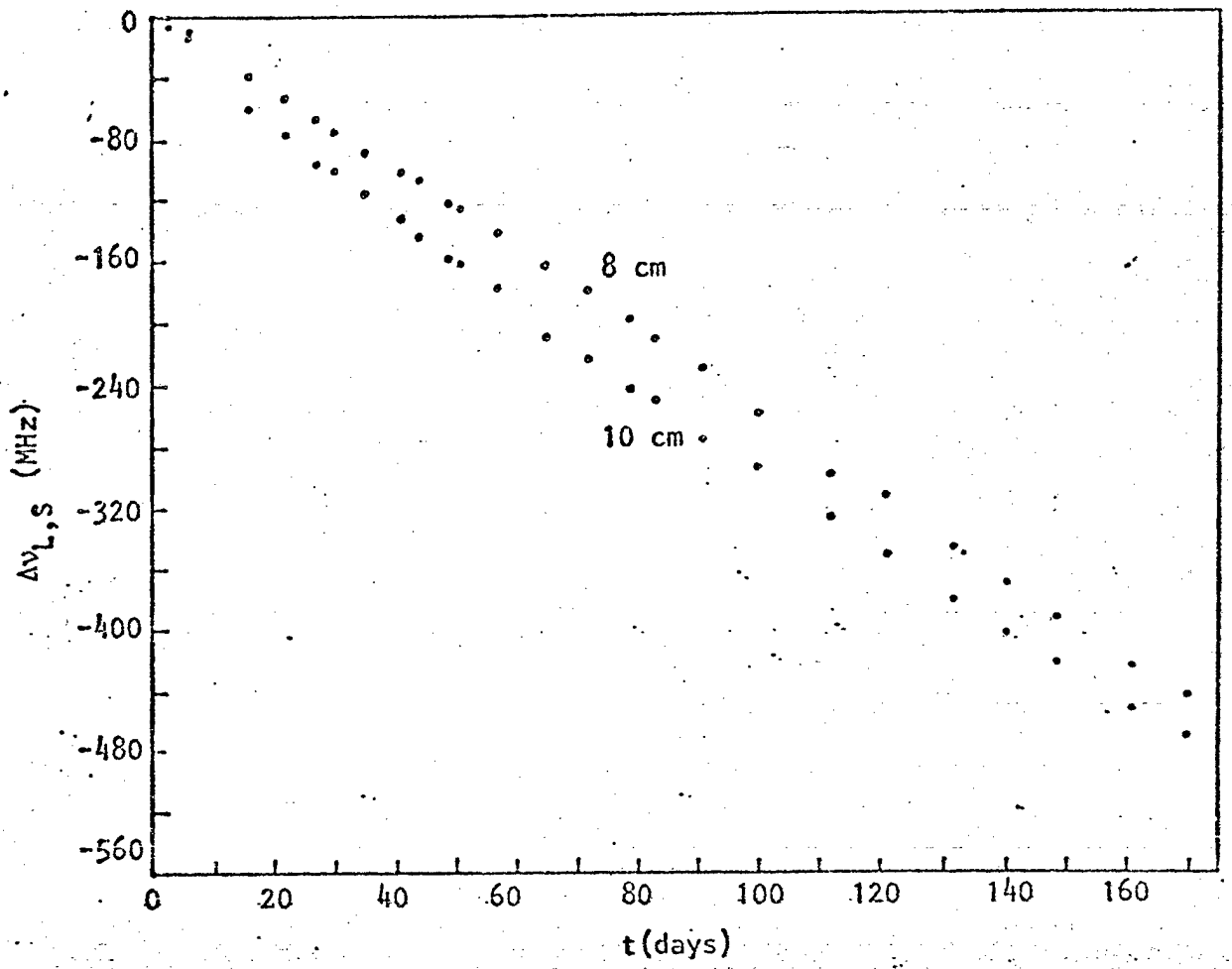
0
-80
-160
-240
-320
-400
-480
-560
$\Delta\nu_{L,S}$ (MHz)
8 cm
10 cm
0
20
40
60
80
100
120
140
160
t (days)

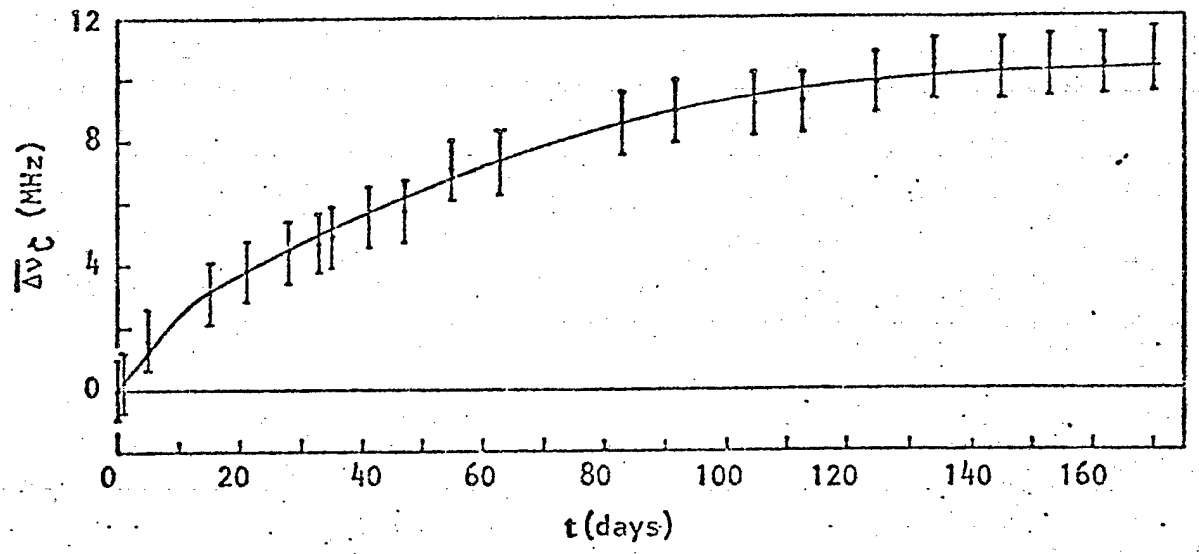
12
8
4
0
$\overline{\Delta\nu_c}$ (MHz)
0
20
40
60
80
100
120
140
160
t (days)

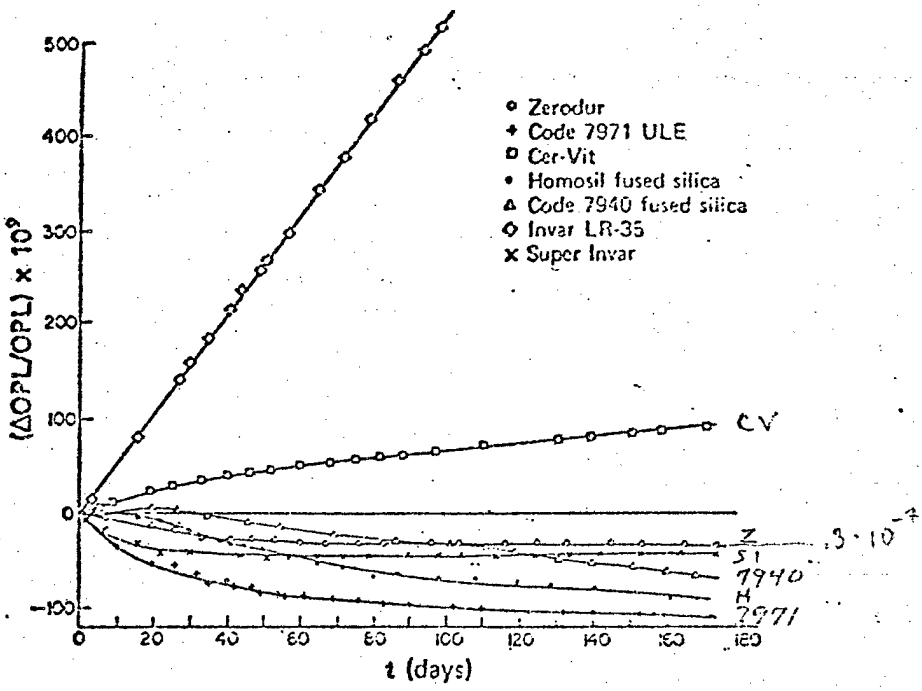
500
400
300
200
100
0
-100
(ΔOPL/OPL) x 10⁹
0
20
40
60
80
100
120
140
160
t (days)
Zerodur
Code 7971 ULE
Cer-Vit
Homosil fused silica
Code 7940 fused silica
Invar LR-35
Super Invar
CV
Z
51
7940
H
7971
3 · 10⁻⁴